Pollen Germination as a High-Throughput Phenotyping Tool for Assessing Heat Tolerance in Soybean

Dheeraj Chatti

dheerajc@ksu.edu

Kansas State University

Aliva Bakshi

Kansas State University

Doina Caragea

Kansas State University

Vara Prasad P. V.

Kansas State University

William. T. Schapaugh

Kansas State University

Article

Keywords: Soybean, Heat stress, Reproductive physiology, Pollen germination, High throughput phenotyping, Machine learning, Deep learning, Object detection, YOLO model

Posted Date: July 1st, 2026

DOI: https://doi.org/10.21203/rs.3.rs-9916027/v1

Additional Declarations: No competing interests reported.

Version of Record: A version of this preprint was published at Scientific Reports on August 18th, 2026.
See the published version at https://doi.org/10.1038/s41598-026-65886-7.

Pollen Germination as a High-Throughput Phenotyping Tool for Assessing Heat Tolerance in Soybean

Dheeraj Chatti [1*], Aliva Bakshi [2], Doina Caragea [2], Vara Prasad P.V. [1], William. T. Schapaugh, Jr. [1]

[1] Department of Agronomy, Kansas State University, Manhattan, Kansas, 66506, USA,

[2] Department of Computer Science, Kansas State University, Manhattan, Kansas, 66506

*Correspondence: Dheeraj Chatti., dheerajc@ksu.edu

Abstract

Background

High temperatures during the reproductive stage of soybean severely disrupt reproductive processes and reduce yield. Heat stress causes ultrastructural damage in pollen grains, leading to reduced pollen germination, pollen size and shortened pollen tube length, ultimately lowering seed set and yield. This experiment aimed to evaluate pollen germination as a reliable, scalable phenotyping tool for assessing male gametophytic tolerance to high temperature stress in soybean. Sixteen soybean breeding lines (genotypes) were grown under controlled environments at optimal (28/18°C; day/night) and high temperature (38/28°C; day/night) regimes during flowering. In vitro pollen germination was quantified using a deep learning–based object detection tool to reduce the manual labor and improve accuracy. Several advanced object detection models belonging to the YOLO (You Only Look Once) family, specifically, YOLOv7–YOLOv12, were evaluated to identify the most reliable model.

Results

Comparative evaluations of different object detection models indicated that YOLOv9 model achieved superior performance in evaluating pollen germination relative to other YOLO models, especially for detecting germinated and non-germinated pollen in complex images. High temperature significantly reduced mean pollen germination from an average of 40% under optimal conditions to an average of 21% under heat stress ($P < 0.05$), with a significant genotype × temperature interaction. Pollen germination across incubation temperatures from 10 °C to 45 °C revealed a defined thermal response; however, no significant interaction between genotypes and incubation temperatures was detected under either growth environment. Although photosynthetic and physiological traits were measured exploring their relationship with pollen germination, their transient and complex response limited their reliability for predicting reproductive performance. The developed image detection tool substantially reduced the time required to evaluate pollen germination. The model processed nearly 5,000 images in approximately one hour, enabling truly high-throughput analysis while minimizing human error.

Conclusions

Findings of this study highlight pollen germination as a practical screening trait for soybean breeding programs aimed at improving heat stress resilience. The integration of deep learning models and high-throughput image-based phenotyping enabled efficient and objective estimation of pollen germination to evaluate male gametophytic heat tolerance in soybean.

Keywords: Soybean, Heat stress, Reproductive physiology, Pollen germination, High throughput phenotyping, Machine learning, Deep learning, Object detection, YOLO model.

Background

Soybean (*Glycine max* (L.) Merr.) is one of the most widely cultivated oilseed crops worldwide. It ranks as the fourth most important crop in terms of seed production, with 353 million tons produced in 2020 [1]. In the United States, soybean is second only to corn in planted area, accounting for 32% of total cultivated land and is a leading oilseed crop adapted to a wide range of climatic conditions.

Temperature is a critical factor regulating plant growth and development [2]. Global mean surface temperatures are projected to rise by approximately 0.3 °C per decade, reaching an increase of 1.5 °C by 2050 and up to 4 °C by 2100 [3]. These increases, driven by anthropogenic climate change, represent one of the most significant abiotic stressors threatening crop survival and productivity [4]. Elevated temperatures during the growing season, even near the optimum range, have already resulted in yield losses in major crops including wheat, maize, rice and soybean [5].

Episodes of extreme heat and heatwaves occur periodically across major soybean-producing regions worldwide, increasing the risk of yield losses [6] [7]. Observational studies indicate that mean temperatures in many soybean-growing areas have risen over the past century, and climate-related trends have been associated with measurable impacts on crop productivity [8]. Modeling analyses further suggest that global soybean yields may decline by approximately 3% per 1 °C increase in temperature in the absence of adaptive management or genetic improvement [9].

In C3 plants such as soybean, high temperature directly reduces the photosynthetic rate by increasing photorespiration. At the physio-biochemical level, elevated temperatures can denature

proteins, enhance lipid fluidity in cell membranes, and promote the accumulation of reactive oxygen species (ROS), ultimately impairing the photosynthetic apparatus. In comparison to the vegetative stage, soybean plants at the reproductive stage are more sensitive to increased temperature, as the optimum temperature for the reproductive stage is lower than that for vegetative growth [10]. Exposure to heat stress above 30°C during the reproductive period often results in reproductive failure and severe yield losses [11,12, 13].

High temperatures during flowering, or even short episodes of heat during pollen release and germination, can disproportionately affect male reproductive processes. Pollen grains are essential for plant fertility and crop productivity, as they deliver male gametes to the embryo sac to achieve double fertilization [14]. Heat stress during flowering has been shown to impair pollen germination, pollen tube growth, and fertilization in several crops [15]. In groundnut, elevated temperatures significantly reduced pod yield, flower production, and the proportion of flowers [16]. Similarly, pollen abnormalities were reported in soybean [17] and common bean [18] under high temperature conditions. However, pollen sensitivity to heat stress varies among species and depends on the specific thermal regime [19].

Accurate phenotyping for heat tolerance during the flowering stage is essential to identify genotypes capable of sustaining reproductive success and yield stability under elevated temperatures. Traditional approaches have focused largely on photosynthetic parameters; however, these traits are highly variable and less directly linked to reproductive outcomes. In contrast, pollen germination has emerged as a biologically relevant and yield-predictive indicator of thermotolerance. Several studies have demonstrated the robustness of pollen viability and germination as phenotyping traits for heat stress. Unlike photosynthetic traits, pollen germination is less influenced by short-term environmental fluctuations and provides a cumulative assessment

of heat exposure during the reproductive phase. Evidence from multiple crops, including soybean, chickpea, wheat, and common bean, shows that pollen germination percentage under high temperature stress strongly correlates with seed set and overall thermotolerance classification [20, 21, 22].

Despite its biological relevance, in vitro pollen germination assessment is labor-intensive, time-consuming and inherently low throughput. Manual counting of germinated pollen grains is also prone to human error and bias [23]. Such limitations hinder the scalability of pollen-based phenotyping in breeding programs that require the evaluation of hundreds or thousands of genotypes under diverse environmental conditions.

Recent advances in high-throughput phenotyping (HTP) and machine learning (ML) provide promising solutions to these challenges. Image-based platforms integrated with machine learning algorithms can rapidly and objectively quantify pollen viability and germination across large sample sets with minimal human intervention [24, 25]. YOLO (You Only Look Once) models operate as single-stage object detectors that simultaneously predict bounding boxes and classify objects in a single pass over the image, rather than performing separate steps for region proposal (object localization) and object classification. The latest YOLO models have been proven to be efficient in terms of both accuracy and speed, and are known to be some of the most efficient real-time detectors. Hence, an optimized real-time pollen germination detection tool can be developed using YOLO models.

However, the utility of this approach for evaluating reproductive heat tolerance in soybean germplasm has not been comprehensively tested. Therefore, this study was designed to integrate controlled-environment stress evaluation with automated image analysis to assess the feasibility of pollen germination as a scalable screening trait.

Objectives

- Quantify variation in pollen germination among soybean breeding lines under optimal and elevated temperature regimes.
- Develop and evaluate a machine learning–based image analysis pipeline for automated pollen germination quantification.
- Assess the physiological responses associated with post-flowering heat stress and examine their relationship with pollen germination.
- Evaluate the potential of image-based pollen germination as a scalable phenotyping tool for reproductive heat tolerance screening.

Methods

Experimental setup and pollen germination

Pollen germination of 16 soybean breeding lines (genotypes), i.e., G2, G3, G5, G6, G7, G8, G9, G12, G13, G14, G17, G18, G21, G22, G23, G24 was evaluated under controlled conditions. Plants were grown in pots containing a standard potting mixture and maintained in growth chambers (CONVIRON) under two temperature regimes during flowering: an optimum regime (28/18°C; day/night) and a high temperature regime (38/28°C; day/night) (Fig. 1). Both growth chambers were maintained under optimal temperature conditions during the vegetative stage. At the onset of flowering in 50% of the plants, one chamber was transitioned to a high-temperature regime, while the other was maintained under the optimal temperature treatment. To ensure adequate exposure to heat stress, pollen collection was initiated after three days of high-temperature treatment and the treatment was maintained for the remainder of the

experiment with continuous water supply. For each genotype, three pots each containing one plant were established as biological replicates. The photoperiod was maintained at 14 hours with a photosynthetic photon flux density (PPFD) of 800–1400 µmol $m^{-2} s^{-1}$. To assess pollen germination, flowers with slightly opened corollas were collected at anthesis (07:00 AM to 09:00 AM). Two to three flowers were collected from each replication and the collected flowers were air-dried for 30 minutes at 25°C. Flower petals were gently opened using forceps and pollen grains were dusted onto glass slides coated with germinating medium by brushing anthers with a nylon hairbrush. The germination medium was prepared by dissolving 15 g of sucrose, 0.03 g of calcium nitrate, and 0.01 g of boric acid in 100 ml of deionized water [11]. To this solution, 0.5 g of agar was added and gently heated on a hot plate. After the agar was completely dissolved, approximately 2 ml of the germinating medium was poured onto clean glass slides and cooled for about 15 min to allow solidification. Slides with pollen grains were placed in empty Petri dishes lined with moistened filter paper to maintain humidity and incubated for 30 min at temperatures ranging from 10 °C to 45 °C in 5 °C increments in eight different incubators (Echotherm, Torrey Pines Scientific, Inc., Carlsbad, CA, USA).

Pollen was visualized on the glass slide using a compound light microscope (Olympus BX51) with an attached camera (Olympus DP70) attached. Pollen germination of 16 genotypes under two temperature treatments was assessed at eight incubation temperatures across three replications. For each slide, 5 to 7 images were captured from randomly selected fields, where 100 to 200 pollen grains were counted (Fig. 2). A pollen was considered to have germinated if the pollen tube length exceeded the pollen grain diameter [20]. Germination percentage was calculated as

$$\text{Germination } \% = \frac{\text{Number of germinated pollen}}{\text{Number of total pollen}} * 100$$

Fig 1. Soybean plants growing in growth chamber

The experiment was divided into two subsets of eight genotypes each, established across two planting dates to facilitate accurate and manageable evaluation. On each experimental day, eight genotypes were assessed under two growth temperature treatments and three incubation temperatures. Completing all eight incubation temperatures for one subset across three replications required eight days. This staggered design enabled efficient organization of the experiment and ensured that all evaluations were conducted within the peak flowering window (R1–R2 stages).

Development of the model

Data annotation:

Data annotation is an important part of developing models to detect and count objects. After images were captured, they were annotated to train and evaluate deep learning models.

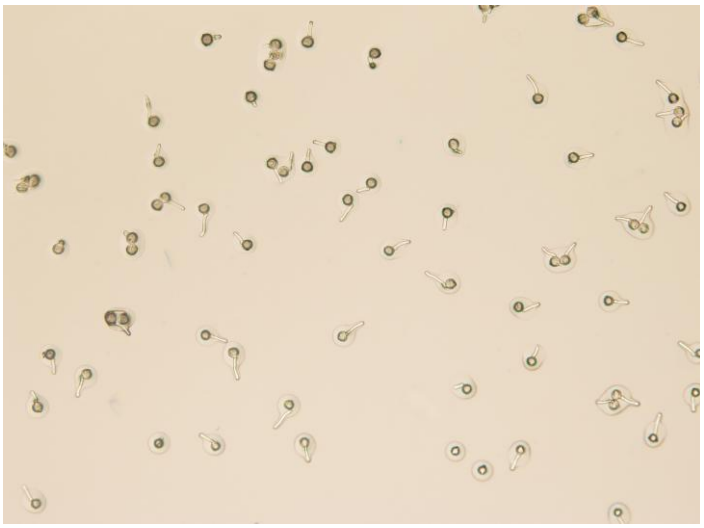

Fig 2. Image of pollen germination

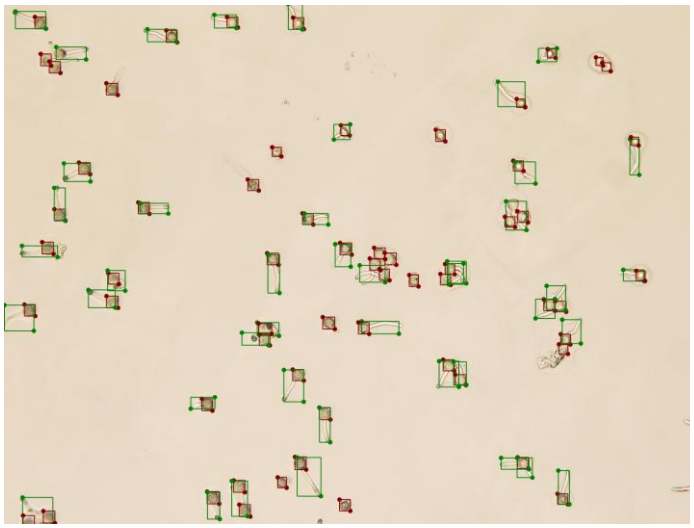

Fig 3. Annotated image of pollen germination. All pollen grains (Red) and germinated pollen grain (Green)

175

176 Annotation was performed using LabelMe, an open-source tool
177 (https://github.com/wkentaro/labelme) that allowed bounding boxes to be drawn and saved as
178 JSON files (Java Script Object Notation). Several strategies were evaluated to determine the most
179 effective approach for pollen annotation to train the ML models. In the final method adopted, we
180 annotated every pollen grain (germinated and non-germinated) as *pollen* and annotated the
181 *germinated pollen* along with the tubes separately. Precise bounding box annotations were
182 created for the two categories as shown in Fig. 3, where the red boxes mark all the *pollen* grains
183 (with and without a germination tail) and the green boxes mark only the *germinated pollen*
184 grains. The number of *non-germinated pollen* grains was then obtained as the difference between
185 the total *pollen* grain count and the *geminated pollen* grain count. This strategy worked the best
186 with our models.

187

Counting by detection workflow:

After annotation, the dataset was split into training, validation, and test sets (Fig. 4). In total, 260 images were annotated covering different genotypes, temperature conditions and incubation temperatures. Of these, 150 images were used for training, 50 images for validation, and 60 images for testing. The three subsets are mutually exclusive, sharing no images. Furthermore, the test set does not overlap with the training or validation sets in terms of genotypes. To achieve effective model performance, the training set was curated to represent the full complexity of the dataset, ranging from clearly separated pollen grains to dense clusters and spiral pollen tubes. The validation set was designed to resemble the test set and anticipated future images, helping to optimize hyperparameters and improve the model's ability to generalize unseen test data. The test set was kept separate to ensure the model was evaluated on unseen data, thereby providing an unbiased assessment.

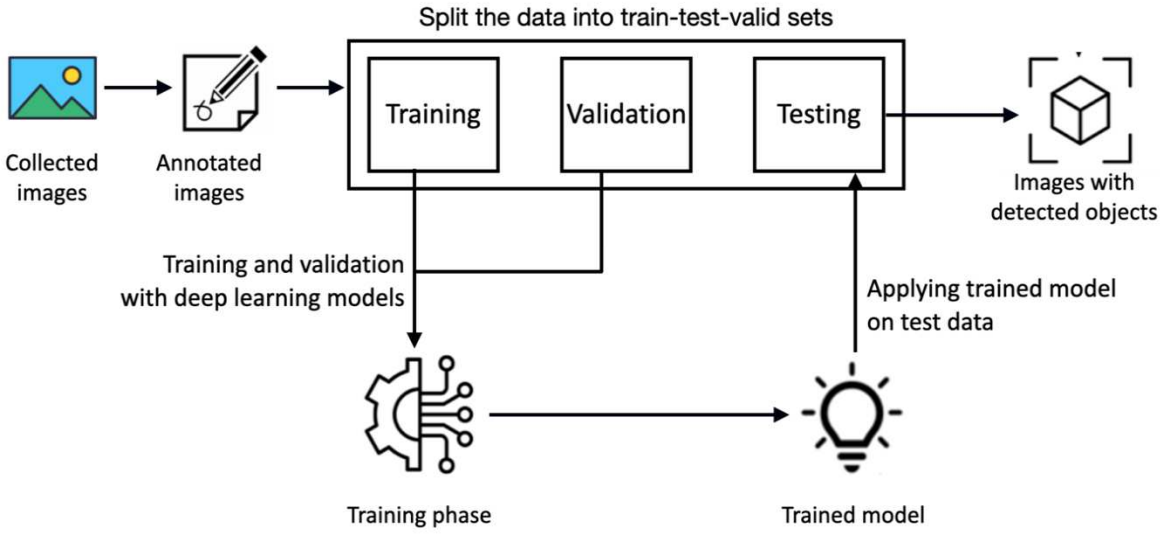

Fig. 4. General workflow for counting by detection models

Supervised object detection:

For pollen counting, a deep learning-based object detection approach was adopted [26]. Several supervised object detection/counting models in the YOLO family were fine-tuned on our dataset, including YOLOv7 [27, 28], YOLOv8, YOLOv9 [29], YOLOv10 [30], YOLOv11 and YOLOv12 [5]. These models were trained to detect and count both pollen grains and germinated pollen grains in each image.

For each YOLO version, we initialized the models with pre-trained weights and fine-tuned them by optimizing select hyperparameters, including the learning rate, IoU threshold, and probabilities for data augmentation, such as mosaic, mixup, and copy-paste. Image resolutions varied across YOLO versions and were selected based on the available GPU (Graphics Processing Unit) memory and the original resolution of our dataset images. We retained the default maximum of 300 objects per image, as no image in our dataset exceeded this limit. All models were trained on 150 images and validated on a separate set of 50 images for 3000 epochs. An early stopping patience of 300 epochs was applied to all YOLO versions. Finally, the model performance was evaluated on the unseen test set using a confidence threshold of 0.25.

Measurement of physiological parameters

Physiological parameters were measured during the flowering stage under optimum and high temperature conditions in three replications. The third uppermost fully opened trifoliate was used for the photosynthetic and biochemical measurements after three days of high temperature treatment. Canopy temperature was measured with the handheld infrared temperature sensor (FLIR Systems AB). Photosynthetic measurements like photosynthetic rate (A)

and stomatal conductance (g_s) were recorded with a portable photosynthesis system (LICOR; LI-6800). Chlorophyll content was recorded with a handheld SPAD meter (Konica Minolta SPAD-502 Plus), and chlorophyll fluorescence (*Fv/Fm*) was measured with a handheld FluorPen (FP100).

Membrane leakage was estimated by determining electrolyte leakage. To eliminate contamination caused by sampling, 10 leaf discs from each subgroup were excised and thoroughly washed with double-distilled water [31]. The samples were transferred to a test tube containing 20 mL of deionized H_2O at 25°C, and the electrical conductivity (*E*0) of the solution was immediately measured with an electrical conductivity meter (DDSJ-308A, Shanghai). After 24 h of incubation at 35°C, the electrical conductivity (*E*1) was measured again. The tubes were then submerged in a 120°C water bath for 20 min. The electrical conductivity (*E*2) was measured after the tubes cooled to 25°C. The percentage of electrolyte leakage (*EL%*) of leaf cells was calculated as follows:

$$EL\% = (E1 - E0) / (E2 - E0) \times 100.$$

Statistical analysis

The experiment followed a factorial completely randomized design with genotype, growth temperature, and incubation temperature treated as main factors. Experimental run and biological replications were included as random factors. Pollen germination data were analyzed using linear mixed-effects models implemented in R (v4.3.1; *lme4* package). The statistical model for pollen germination (*PG*) was:

$$PG_{ijkl} = \mu + G_i + T_j + I_k + (G \times T)_{ij} + (G \times I)_{ik} + (T \times I)_{jk} + (G \times T \times I)_{ijk} + R_l + \varepsilon_{ijkl}$$

where G_i represents genotype, T_j growth temperature regime, I_k incubation temperature, R_l experimental run (random effect), and ε_{ijkl} the residual error. Significance was assessed at $P < 0.05$, and mean separation was conducted using Tukey-adjusted comparisons when appropriate. Heat maps were generated using the *ComplexHeatmap* package, and Pearson correlation coefficients were calculated and visualized using the *metan* package in R.

Results & Discussion

Model performance

For object detection models, performance is typically evaluated using mean Average Precision (mAP), which is defined as the area under the precision-recall curve averaged across categories (in our case, *pollen* and *germinated pollen* grains). It is calculated by using the Intersection over Union (IoU) metric, which measures the overlap between the predicted bounding box and the manually annotated bounding box of an object. For example, an IoU of 0.50 indicates that there is at least 50% overlap between predicted and annotated bounding boxes. Different mAP values can be obtained for different IoU thresholds. In this study, model performance was evaluated using AP@0.50, AP@0.75 and mAP@ [0.50:0.95] (the average of AP values from 0.50 to 0.95, with a step of 0.05).

The performance of different object detection YOLO models on the test set is summarized in Table 1. The test images were selected to be both representative of the data distribution and challenging for the models. These images were not seen by the models during training or validation, and there is no overlap between genotypes in the test set and those in the training and validation sets. Among the models trained, the YOLOv9 model demonstrated more consistent and superior performance across varying levels of image complexity.

Table 1. Performance evaluation of different models on test set

Model	mAP	mAP@50	mAP@75
YOLOv7	59.7	77.2	72.1
YOLOv8	66.5	82.9	78.5
YOLOv9	**72.2**	**86.3**	**83.6**
YOLOv10	67.5	83.1	79.2
YOLOv11	69.7	84.7	80.0
YOLOv12	69.2	84.6	80.3

Table 2 demonstrates predictions made by various YOLO models on a small representative sample of images from our test dataset. The results indicate that YOLOv9 emerged as the most reliable and accurate model among the tested versions. It achieved the best average accuracy in predicting the percentage of germinated pollen grains, did not introduce false positives in zero-germination cases, and maintained stable performance across both low and high germination scenarios. Based on these observations, YOLOv9 was considered the most dependable model to be used for large-scale detection of pollen germination percentage.

Table 2. Comparison between pollen germination (%) detection by each model on several control (CONT) and treatment (TRT) images representative of the test set. (g: germinated pollen, p: total number of pollen grains)

Image	Manual Count	YOLOv7	YOLOv8	YOLOv9	YOLOv10	YOLOv11	YOLOv12
40.5.8 G 40 TRT	0%, 0g, 61p	1.64%. 1g, 61p	0%, 0g, 63p	0%, 0g, 61p	0%, 0g, 61p	0%, 0g, 62p	0%, 0g, 62p
45.6.4 G 45 TRT	37.36%, 34g, 91p	13.97%,13g, 93p	13.99% 13g, 93p	19.78%,17g, 86p	15.38%, 14g, 91p	11.96%, 11g, 92p	15.38%, 14g, 91p
54.2.5 G 54 CONT	27.27%, 3g, 11p	25%, 3g, 12p	21.43%, 3g, 14p	27.27%,3g, 11p	27.27%,3g, 11p	25%, 3g, 12p	28.57%, 8g, 27p
3.6.3 G 3 TRT	31.58%, 12g, 38p	28.21%,11g, 39p	15.34%, 6g, 39p	18.00%, 7g, 39p	17.94%, 7g, 39p	14.63%, 6g, 41p	15%, 6g, 40p
6.5.1 G 6 CONT	12,5%, 3g, 24p	12.5%, 3g, 24p	4.17%, 1g, 24p	13.0%, 3g, 23p	8.33%, 2g, 24p	13.04, 3g, 23p	12.5%, 3g, 24p

Overall, our experiment generated more than 5,000 images of pollen germination. Manually counting pollen germination at 2–3 minutes per image would require nearly 250 hours of labor, not including fatigue, cost, and inherent human error and inconsistencies. In contrast, the developed image detection model analyzed the entire dataset within 30 minutes to 1 hour, transforming a time-consuming task into a truly high-throughput process. The model also reduced potential human error and inconsistencies due to fatigue and automatically output pollen germination percentages for each replication, along with mean average precision values ready for statistical analysis through automated Python software. We also tested our best model on pollen images from other crops to assess its transferability and robustness. Preliminary tests on other crop species, such as chickpea and cherry, showed promising results, suggesting potential adaptability to additional crops, although further validation is required (data not shown).

Pollen germination

High temperature stress significantly reduced pollen germination in soybean breeding lines (genotypes) (Fig. 5), with reductions of up to 47% compared to the control. At the extreme incubation temperature of 45 °C, pollen grains appeared shattered and failed to germinate. Likewise, no germination occurred at 10 °C and 15 °C (data not shown). Because these temperatures consistently resulted in no pollen germination, these temperatures were excluded as zero variance precluded statistical comparison. Across genotypes, the highest pollen germination rates were observed at incubation temperatures of 25 °C, 30 °C, and 35 °C under both control and high-temperature treatments, identifying this range of incubation temperatures as optimal for soybean pollen germination (Fig. 6). Analysis revealed a significant interaction between genotype and temperature ($P < 0.05$) for pollen germination, however the interaction between genotype and incubation temperature was not significant. Therefore, the mean pollen germination (%) for each genotype was determined by averaging values obtained under five incubation temperatures (20°C, 25°C, 30°C, 35°C, 40°C) across three replications. Among the evaluated lines, breeding line G2 recorded the highest mean pollen germination (50%), while G18 recorded the lowest (15%) under combined high and control temperature treatments (Table 3). Genotypes G24 and G2 exhibited the lowest percent reductions in pollen germination under high temperature compared to the control, with reductions of 3% and 5%, respectively. However, while G24 showed minimal reduction, its absolute germination remained consistently low across both temperature regimes. In contrast, genotypes G22 and G8 were highly susceptible to high temperature, with germination declining from 53% to 11% and from 42% to 10%, respectively. Genotype G2 stood out as the most stable, maintaining consistently high pollen germination under both optimal and high-temperature conditions, underscoring its potential for heat-tolerant breeding strategies.

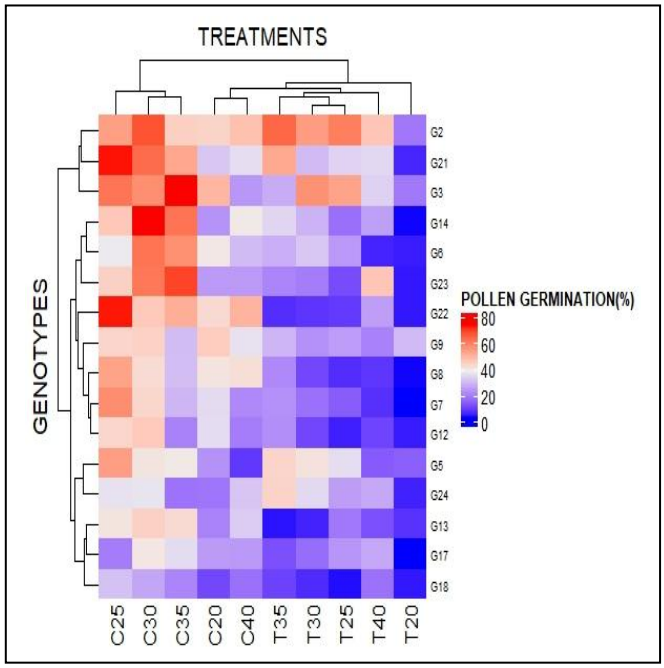

Fig 5. Heat map showing the pollen germination (%) of soybean genotypes across the incubation temperatures (20, 25, 30, 35, 40^0 C) at control [C] ($28/18^0$C) and high temperature [T] ($38/28^0$C)

These results align with previous research showing that heat stress delays and reduces pollen germination and shortens pollen tube growth in cotton [32], soybean [12, 33] and chickpea [22]. Heat stress has also been reported to impair pollen tube formation and alter pollen tube kinetics [34, 35]. In rice, high temperatures promoted pollen sterility and markedly suppressed pollen germination [36]. Similarly, in soybean, higher temperatures extended the duration of flowering, while reducing pollen germination, pollen size and pollen tube length, ultimately leading to yield loss [37].

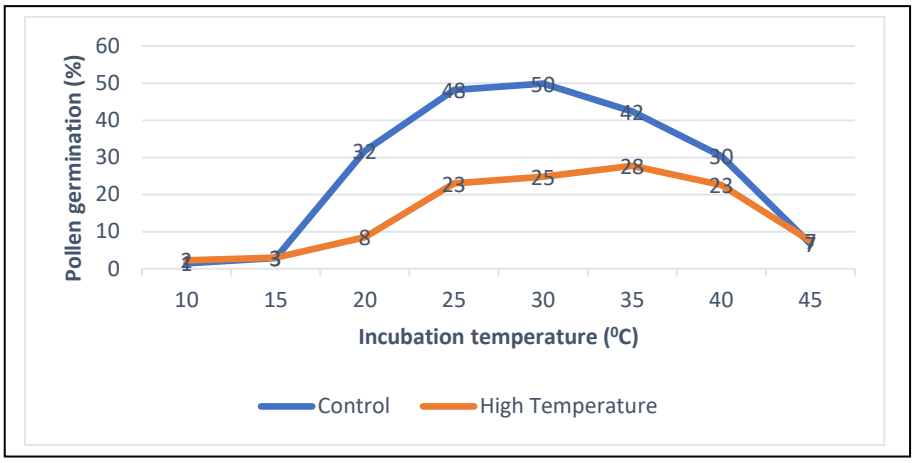

Fig 6. Pollen germination (%) of soybean genotypes at various incubation temperatures under control (28/18^{0}C) and high temperature (38/28^{0}C).

Physiological Parameters

Significant changes were observed in canopy temperature, stomatal conductance, photosynthesis, chlorophyll fluorescence, chlorophyll content, and membrane integrity, providing a comprehensive view of plant adaptive and stress responses under elevated temperatures (Fig. 7). Canopy temperature increased significantly under the high temperature treatment (34.7°C) compared to the control (26.6°C), with a significant genotype - treatment interaction, highlighting genotype specific responses to heat stress. Stomatal conductance (g_s) also increased significantly by approximately 89% under high temperature, indicating enhanced transpiration cooling, supported by the well-watered conditions throughout the experiment. Although this active transpiration likely improved tolerance, it was insufficient to reduce canopy temperature below 32°C, suggesting a limitation in cooling capacity under extreme heat. The interaction between the temperature treatments and genotypes was also statistically significant (P<0.05) for stomatal conductance.

Photosynthesis is a key indicator of plant growth because of its link to crop productivity. Elevated temperature can influence photosynthesis through both stomatal and non-stomatal mechanisms. In this study, the photosynthetic rate was significantly higher in the high-temperature treatment, showing a 97% increase compared to the control. But no significant interaction was found between genotypes and temperature treatments. This is contrary to the previous findings, which showed that high temperatures decreased leaf photosynthetic rate and stomatal conductance by hampering net photosynthesis [38, 17].

Chlorophyll fluorescence (*Fv/Fm*) is commonly used as an indicator of the maximal photochemical efficiency of photosystem II (PSII) and serves as a measure of plant health and photosynthetic efficiency. In this experiment, *Fv/Fm* declined significantly by 7 % under high temperature conditions compared to the optimum, although no significant interaction was detected between genotype and temperature treatments.

372

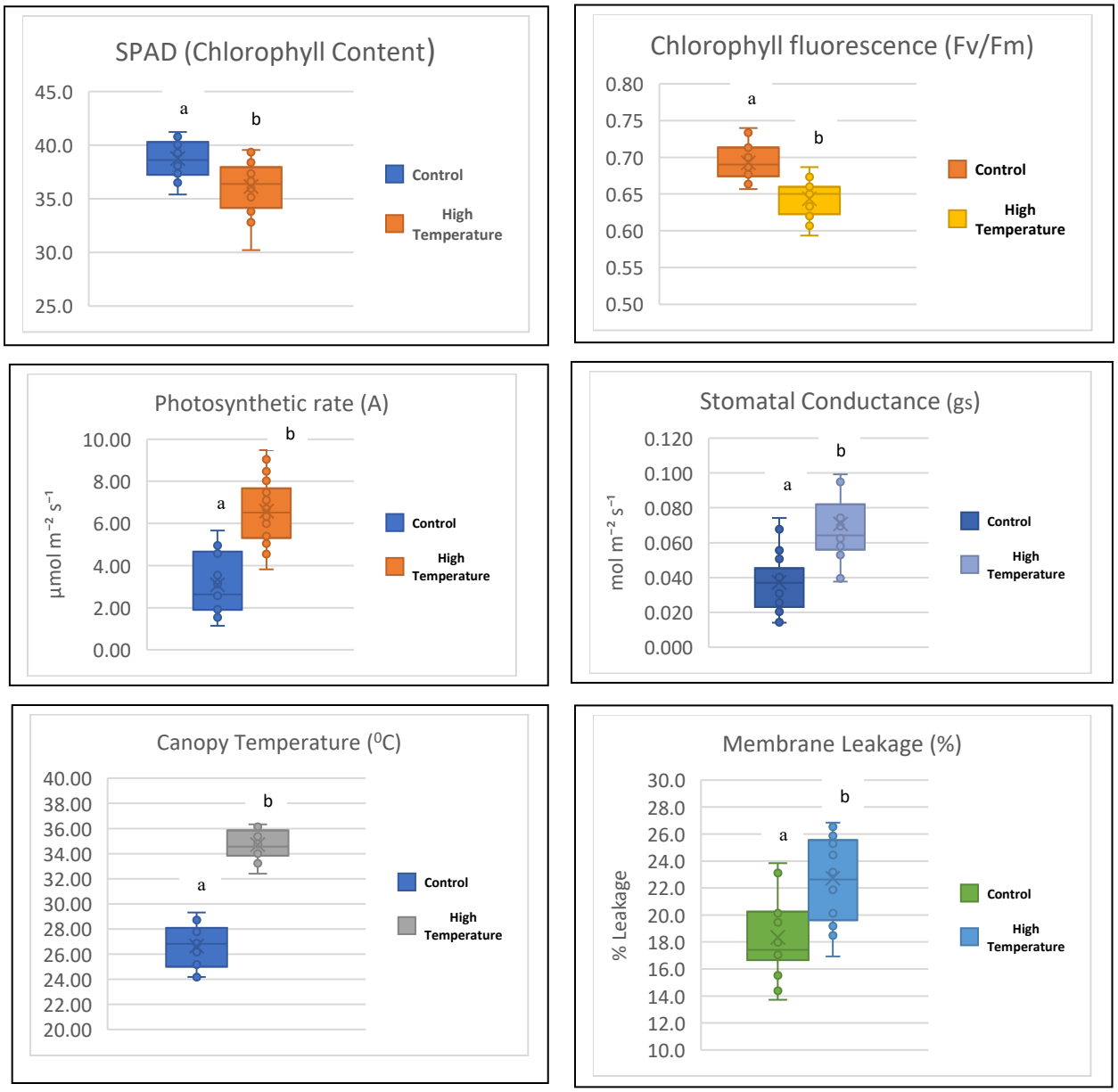

Fig 7. Physiological parameters of soybean genotypes grown under control (28/18^{0}C) and high temperature (38/28^{0}C) environments. Different letters on the boxes indicate statistically significant differences between treatments (P<0.05)

373

374

375

Table 3. Mean pollen germination (%) of soybean genotypes under optimum (28^0C/18^0C) and high temperature (38^0C/28^0C) conditions.

376

Breeding line (Genotype)	Optimum temperature (28^0C/18^0C)	High temperature (38^0C/28^0C)	Mean
G2	52a	49a	50
G3	54a	38a	46
G5	33a	30a	31
G6	45a	19b	32
G7	37a	13b	25
G8	42a	10b	26
G9	40a	25b	33
G12	33a	11b	22
G13	36a	10b	23
G14	50a	22b	36
G17	29a	16a	23
G18	21a	8b	15
G21	51a	31b	41
G22	53a	11b	32
G23	45a	21b	33
G24	28a	27a	28
Mean ± SE	40±4.35	21±1.53	

Means within a row, followed by the same letter are not significantly different (P=0.05 level).
SE = Standard Error of mean

377 Previous studies on chlorophyll fluorescence in soybean under abiotic stress have largely
378 focused on *Fv/Fm* [39, 40]. High temperatures induce denaturation and conformational changes in
379 PSII core proteins, particularly the D1 protein, which is essential for primary electron transfer

reactions. Heat stress accelerates D1 protein degradation while simultaneously impairing its repair and resynthesis, resulting in the accumulation of damaged PSII complexes [41].

The concurrent observation of higher photosynthetic rate, increased stomatal conductance, and reduced *Fv/Fm* under high temperature conditions represents a complex interplay of adaptive and stress responses in plants. Elevated stomatal conductance (g_s) under heat stress promotes enhanced transpiration, facilitating leaf cooling and sustaining CO_2 diffusion into the mesophyll, thereby maintaining or even increasing the net photosynthetic rate (A) [42, 43]. This suggests that the gas exchange system remained functional, as plants were maintained under well-watered conditions and grown under optimal temperatures until flowering, while the photosynthetic rate was measured only three days after the initiation of high-temperature stress. Under these conditions, the system may confer a compensatory advantage against thermal damage. In contrast, the simultaneous reduction in *Fv/Fm*, an indicator of the maximum quantum efficiency of Photosystem II (PSII), signals photoinhibition or heat-induced stress within the photosynthetic electron transport chain [44, 45]. Such a response indicates that while the plant is actively assimilating carbon, the photochemical efficiency of PSII is compromised, possibly due to damage to the D1 protein, impaired PSII repair mechanisms, or the accumulation of reactive oxygen species (ROS) [46, 47].

This physiological uncoupling, where the light reactions are partially inhibited but the carbon fixation pathway remains robust, is often reported in heat-tolerant genotypes and may represent a short-term survival strategy [42, 44]. Plants in this state may rely on increased energy dissipation through non-photochemical quenching (NPQ), photorespiration, and heat shock protein activity to protect the photosynthetic machinery and maintain function

[48]. Previous studies reported similar observations in cereals and legumes, including wheat [44, 49], cowpea [45] and tomato [46].

The SPAD chlorophyll meter is widely used as an indirect measure of leaf chlorophyll content in plants [9]. In this study, mean SPAD values ranged from 30 to 42, suggesting significant variation in leaf chlorophyll content due to the temperature treatments, genotypes and their interaction. High temperature treatment significantly reduced chlorophyll content by 7.2% compared to the control. This decline supports earlier work reporting reduced chlorophyll under heat stress in several crops [49, 50]. A decline in chlorophyll content has also been associated with suppressed chlorophyll fluorescence [51]. The observed decrease in SPAD readings, may reflect direct effects of high temperature stress on chloroplast membranes and PSII function in plants as shown in tomato [52] and chickpea [22].

High temperatures disrupt the structural integrity of the thylakoid membranes, increasing membrane fluidity and potentially causing ion leakage and impaired proton gradients [53, 42]. In this study, this effect was evident from a significant increase of 24% in membrane leakage under high temperature conditions. At 38/28°C, heat stress distorted the plasma membrane, as well as chloroplast, thylakoid and mitochondrial membranes, including cristae and matrix structures, compared to the normal growth temperature (28/18°C) [38].

Phenotyping for heat stress tolerance during soybean reproductive stages remains a major challenge due to the complexity and variability of physiological responses. In this study, most physiological traits showed no strong or consistent correlations, indicating substantial variation in plant responses and the influence of both genotypic and environmental interactions (Fig. 8).

A positive correlation was observed between photosynthetic rate (A) and stomatal conductance (g_s), consistent with the interdependence of gas exchange and carbon assimilation. Increased stomatal aperture under high temperatures facilitates CO_2 influx, thereby maintaining or enhancing photosynthesis [42]. However, this compensatory response does not necessarily indicate stress resilience, as it may mask underlying photoinhibition or damage to other photosynthetic components. Indeed, despite the maintained or increased photosynthetic rates, plants still exhibited reduced chlorophyll fluorescence and increased membrane leakage, revealing cellular stress under high temperature conditions.

Pollen germination (PG) showed a weak negative correlation with membrane leakage and photosynthetic rate (A), suggesting that elevated physiological activity under stress does not necessarily translate to reproductive success. This decoupling between vegetative physiological responses and reproductive viability reinforces the idea that conventional parameters such as photosynthetic rate, while important, may not fully capture the extent of stress-induced reproductive failure.

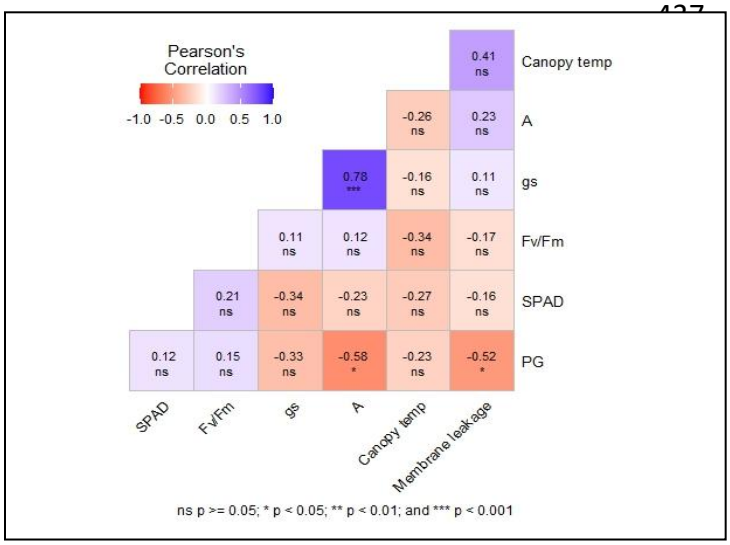

Fig 8. Correlation between various physiological parameters and pollen germination (calculated on averaged data of optimum and high temperature treatments)

In contrast, pollen germination directly reflects the reproductive competence of the plant, which is highly sensitive to elevated temperatures. The negative correlation with membrane leakage supports the critical role of membrane stability for pollen viability, as increased leakage may signify oxidative or thermal damage impairing gametophytic function. Similarly, the inverse trend with photosynthetic rate may indicate that reproductive processes can fail even under apparently "productive" vegetative conditions, consistent with reports of resource allocative shifts or oxidative damage disproportionately affecting the reproductive organs under heat stress [45, 38].

This physiological uncoupling underscores the limitations of relying solely on photosynthetic traits for selecting heat-tolerant genotypes. In contrast, pollen germination offers a more integrative and yield-relevant phenotype, directly linked to pod set and seed formation. Since reproductive failure is often the primary cause of yield loss under heat events, pollen germination provides a robust and biologically meaningful parameter for evaluating thermotolerance. Recent advances in machine learning models can substantially enhance this potential. Models trained on annotated pollen images in this experiment can identify germinated and non-germinated pollen grains and even assess subtle changes in pollen tube lengths. Integrating these tools into pollen germination phenotyping enables rapid, consistent and large-scale screening across field and greenhouse experiments [23, 25]. YOLOv9 [3] introduced novel training mechanisms such as programmable gradient information (PGI) and the generalized efficient layer aggregation network (GELAN) to improve feature learning and detection robustness. It achieves better accuracy and generalization while maintaining real-time performance. These improvements make YOLOv9 effective for detecting small and densely distributed objects like pollen grains.

Conclusion and future prospects

This study revealed significant variation in pollen germination among soybean breeding lines under optimal and elevated temperature regimes, highlighting genotypic differences in reproductive heat tolerance. A machine learning–based image analysis pipeline was developed for automated pollen germination quantification, enabling rapid and accurate analysis of large image datasets. The results indicate that while photosynthetic traits provide insight into physiological responses to heat stress, pollen germination serves as a more direct and yield-relevant indicator of post-flowering heat tolerance. The image-based approach also demonstrates strong potential as a scalable, high-throughput phenotyping tool for screening heat tolerance in breeding programs.

Future research will further investigate the relationship between pollen germination, seed yield, and environmental factors across diverse environments. Integrating these datasets using advanced predictive models may improve the prediction of yield potential and genotype adaptability under future climate scenarios.

List of abbreviations:

A: Photosynthetic rate

AP: Average precision

Fm: Maximum fluorescence

Fv: Variable fluorescence

g_s : Stomatal conductance

HTP: High throughput phenotyping

IoU: Intersection over Union

JSON: Java Script Object Notation

ML: Machine learning

PG: Pollen germination

PPFD: Photosynthetic photon flux density

R – CNN: Region – based convolutional neural networks

SPAD: Soil Plant Analysis Development

YOLO: You Only Look Once

Declarations

Acknowledgements

We gratefully acknowledge the invaluable support provided by the Department of Agronomy, the Department of Computer Science, and the Plant Physiology Laboratory at Kansas State University, Manhattan, USA.

Author contributions

*DC: Conducting the experiment, pollen study, methodology, writing - review, editing, data analysis. AB: Development of machine learning, review, writing, editing. DC: Model curation, supervision, review. VPPV: Funding acquisition, laboratory access, supervision, review. WTS: Project administration, supervision, funding acquisition, conceptualization, writing, review.

Funding

This research was funded by the Kansas State University Agricultural Experiment Station, Corteva Agriscience, and the Kansas Soybean Commission.

Data availability

All data supporting the findings of this study are available within the paper

Ethics approval and consent to participate

Not applicable

Consent for publication

Not applicable

Competing Interests

Authors declared no competing interests

References

1. FAOSTAT: Crops and livestock products: soybean production data. https://www.fao.org/faostat/ (2022). Accessed 15 Feb 2026.

2. Patel D, Franklin KA. Temperature regulation of plant architecture. Plant Signal Behav. 2009;4(7):577–579. doi:10.4161/psb.4.7.8849.

3. Intergovernmental Panel on Climate Change: Summary for Policymakers. In: Global warming of 1.5 °C. https://www.ipcc.ch/sr15/ (2018). Accessed 15 Feb 2026.

4. Nahar K, Hasanuzzaman M, Rahman A, Alam MM, Mahmud JA, Suzuki T, Fujita M. Polyamines confer salt tolerance in mung bean (*Vigna radiata* L.) by reducing sodium uptake, improving nutrient homeostasis, antioxidant defense, and methylglyoxal detoxification systems. Front Plant Sci. 2016;7:1104. doi:10.3389/fpls.2016.01104.

5. Yu C, Miao R, Khanna M. Maladaptation of U.S. corn and soybeans to a changing climate. Sci Rep. 2021;11:12351. doi:10.1038/s41598-021-91192-5.

6. Vogel E, Donat MG, Alexander LV, Meinshausen M, Ray DK, Karoly D, Meinshausen N, Frieler K. The effects of climate extremes on global agricultural yields. Environ Res Lett. 2019;14:054010. doi:10.1088/1748-9326/ab154b.

7. Herritt MT, Fritschi FB. Characterization of photosynthetic phenotypes and chloroplast ultrastructural changes of soybean (*Glycine max*) in response to elevated air temperatures. Front Plant Sci. 2020;11:153. doi:10.3389/fpls.2020.00153.

8. Lobell DB, Asner GP. Climate and management contributions to recent trends in U.S. agricultural yields. Science. 2003;299:1032. doi:10.1126/science.1078475.

9. Zhao C, Liu B, Piao S, Wang X, Lobell DB, Huang Y, Huang M, Yao Y, Bassu S, Ciais P, Durand JL, Elliott J, Ewert F, Janssens IA, Li T, Lin E, Liu Q, Martre P, Müller C, Peng S, Peñuelas J, Ruane AC, Wallach D, Wang T, Wu D, Liu Z, Zhu Y, Zhu Z, Asseng S. Temperature increase reduces global yields of major crops in four independent estimates. Proc Natl Acad Sci USA. 2017;114:9326–9331. doi:10.1073/pnas.1701762114.

10. Li F, Shao Y, Wang Z, et al. Yield compensation among plant regions improves soybean adaptation to short-term high-temperature stress during the reproductive period. J Plant Physiol. 2024;293:154167. doi:10.1016/j.jplph.2023.154167

11. Salem MA, Kakani VG, Koti S, Reddy KR. Pollen-based screening of soybean genotypes for high temperatures. Crop Sci. 2007;47:219–231. doi:10.2135/cropsci2006.07.0443.

12. Djanaguiraman M, Prasad PVV, Schapaugh WT. High day- or nighttime temperature alters leaf assimilation, reproductive success, and phosphatidic acid of pollen grain in soybean (*Glycine max* [L.] Merr.). Crop Sci. 2013;53:1594–1604.

13. Chaudhary S, Devi P, HanumanthaRao B, Jha UC, Sharma KD, Prasad PVV, Kumar S, Siddique KHM, Nayyar H. Physiological and molecular approaches for developing thermotolerance in vegetable crops: a growth, yield and sustenance perspective. Front Plant Sci. 2022;13:878498. doi:10.3389/fpls.2022.878498.

14. Garcia CC, Nepi M, Pacini E. It is a matter of timing: asynchrony during pollen development and its consequences on pollen performance in angiosperms—a review. Protoplasma. 2017;254:57–73.

15. Hall AE. Comparative ecophysiology of cowpea, common bean and peanut. In: Nguyen HT, Blum A, editors. Physiology and biotechnology integration for plant breeding. New York: Marcel Dekker; 2004. p. 271–325.

16. Prasad PVV, Craufurd PQ, Kakani VG. Influence of high temperature during pre- and post anthesis stages of floral development on fruit-set and pollen germination in peanut. Aust J Plant Physiol. 2001;28:233–240.

17. Koti S, Reddy KR, Reddy VR, Kakani VG, Zhao D. Interactive effects of carbon dioxide, temperature, and ultraviolet-B radiation on soybean (*Glycine max* L.) flower and pollen morphology, pollen production, germination, and tube lengths. J Exp Bot. 2005;56:725–736.

18. Suzuki K, Takeda H, Tsukaguchi T, Egawa Y. Ultrastructural study of degeneration of tapetum in anther of snap bean (*Phaseolus vulgaris* L.) under heat stress. Sex Plant Reprod. 2001;13:293–299.

19. Parrotta L, Faleri C, Cresti M, Cai G. Heat stress affects the cytoskeleton and the delivery of sucrose synthase in tobacco pollen tubes. Planta. 2016;243:43–63.

20. Prasad PVV, Boote KJ, Allen LH Jr. Adverse high temperature effects on pollen viability, seed-set, seed yield and harvest index of grain sorghum (*Sorghum bicolor* L. Moench) are more severe at elevated carbon dioxide due to higher tissue temperatures. Agric For Meteorol. 2006;139:237–251.

21. Djanaguiraman M, Prasad PVV, Seppänen M, et al. Role of polyamines in protecting soybean reproductive development against high temperature stress. Environ Exp Bot. 2018;153:39–50.

22. Kaushal N, Awasthi R, Gupta K, Gaur P, Siddique KHM, et al. Heat-stress-induced reproductive failures in chickpea (*Cicer arietinum*) are associated with impaired sucrose metabolism in leaves and anthers. Funct Plant Biol. 2013;40:1334–1349.

23. Andres J, et al. High-throughput phenotyping and machine learning enable the efficient evaluation of pollen viability in crops. Plant Methods. 2021;17:106.

24. Yuan F, et al. High-throughput measurement of pollen viability using machine learning and hyperspectral imaging. Biosyst Eng. 2019;181:163–173.

25. Chen X, et al. Automated pollen analysis using machine learning and computer vision techniques. Comput Electron Agric. 2022;198:107022.

26. Ren S, He K, Girshick R, Sun J. Faster R-CNN: towards real-time object detection with region proposal networks. IEEE Trans Pattern Anal Mach Intell. 2016;39(6):1137–1149.

27. Wang CY, Bochkovskiy A, Liao HYM. YOLOv7: trainable bag-of-freebies sets new state-of-the-art for real-time object detectors. In: Proc IEEE/CVF Conf Comput Vis Pattern Recognit (CVPR). 2023b.

28. Jocher G, Chaurasia A, Qiu J. Ultralytics YOLOv8 [software]. 2023. Available from: https://github.com/ultralytics/ultralytics.

29. Wang Y, Yeh IH, Liao HYM. YOLOv9: learning what you want to learn using programmable gradient information. arXiv. 2024b;arXiv:2402.13616.

30. Tian Y, Ye Q, Doermann D. YOLOv12: Attention-centric real-time object detectors. arXiv. 2025;arXiv:2502.12524.

31. Lutt S, Kinet JM, Bouharmont J. NaCl-induced senescence in leaves of rice cultivars differing in salinity resistance. Ann Bot. 1996;78:389–398. doi:10.1006/anbo.1996.0134.

32. Snider JL, Oosterhuis DM, Kawakami EM. Mechanisms of reproductive thermotolerance in *Gossypium hirsutum*: the effect of genotype and exogenous calcium application. J Agron Crop Sci. 2011;197:228–236.

33. Gogoi N, Farooq M, Barthakur S, Baroowa B, Paul S, et al. Thermal stress impacts on reproductive development and grain yield in grain legumes. J Plant Biol. 2018;61:265–291.

34. Foster J, Lee YH, Tegeder M. Distinct expression of members of the LHT amino acid transporter family in flowers indicates specific roles in plant reproduction. Sex Plant Reprod. 2008;21:143–152.

35. Distefano G, Hedhly A, Las Casas G, La Malfa S, Herrero M, et al. Male–female interactions and temperature variation affect pollen performance in citrus. Sci Hortic. 2012;140:1–7.

36. Zhang C, Li G, Chen T, Feng B, Fu W, et al. Heat stress induces spikelet sterility in rice at anthesis through inhibition of pollen tube elongation interfering with auxin homeostasis in pollinated pistils. Rice. 2018;11:26. doi:10.1186/s12284-018-0206-5.

37. Poudel S, Adhikari B, Dhillon J, Reddy KR, Stetina SR, Bheemanahalli R. Quantifying the physiological, yield, and quality plasticity of Southern USA soybeans under heat stress. Plant Stress. 2023;9:100195. doi:10.1016/j.stress.2023.100195.

38. Djanaguiraman M, Prasad PVV, Boyle DL, Schapaugh WT. High-temperature stress and soybean leaves: leaf anatomy and photosynthesis. Crop Sci. 2011;51:2125–2131.

39. Van Heerden PD, Strasser RJ, Krüger GH. Reduction of dark chilling stress in N_2-fixing soybean by nitrate as indicated by chlorophyll *a* fluorescence kinetics. Physiol Plant. 2004;121(2):239–249. doi:10.1111/j.0031-9317.2004.0312.x.

40. Ohashi Y, Nakayama N, Saneoka H, Fujita K. Effects of drought stress on photosynthetic gas exchange, chlorophyll fluorescence and stem diameter of soybean plants. Biol Plant. 2006;50(1):138–141. doi:10.1007/s10535-005-0089-3.

41. Yamamoto Y, Aminaka R, Yoshioka M, Khatoon M, Komayama K, Takenaka D, et al. Quality control of photosystem II: impact of light and heat stresses. Photosynth Res. 2008;98(1–3):589–608. doi:10.1007/s11120-008-9372-4.

42. Wahid A, Gelani S, Ashraf M, Foolad M. Heat tolerance in plants: an overview. Environ Exp Bot. 2007;61:199–223.

44. Sharma DK, Andersen SB, Ottosen CO, Rosenqvist E. Wheat cultivars selected for high Fv/Fm under heat stress maintain high photosynthesis, total chlorophyll, stomatal conductance, transpiration, and dry matter. Physiol Plant. 2015;153(2):284–298. doi:10.1111/ppl.12245.

45. Ismail AM, Hall AE. Reproductive-stage heat tolerance, leaf membrane thermostability and plant morphology in cowpea. Crop Sci. 1999;39:1762–1768. doi:10.2135/cropsci1999.3961762x.

46. Li X, Li Y, Ahammed GJ, Zhang XN, Ying L, Zhang L, Yan P, Zhang LP, Li QY, Han WY. RBOH1-dependent apoplastic H_2O_2 mediates epigallocatechin-3-gallate-induced abiotic stress tolerance in tomato (*Solanum lycopersicum* L.). Plant Physiol Biochem. 2019;161:357–366.

47. Baker NR. Chlorophyll fluorescence: a probe of photosynthesis in vivo. Annu Rev Plant Biol. 2008;59:89–113.

48. Bita CE, Gerats T. Plant tolerance to high temperature in a changing environment: scientific fundamentals and production of heat stress-tolerant crops. Front Plant Sci. 2013;4:273.

49. Wiley E, et al. Stomatal conductance increases under heat and elevated CO_2 in wheat: a mechanism for maintaining photosynthesis. Plant Cell Environ. 2021;44(6):1857–1871.

50. Kumar S, Kaur R, Kaur N, Bhandhari K, Kaushal N, Gupta K, Bains TS, Nayyar H. Heat stress effects on reproductive development in chickpea. Acta Physiol Plant. 2011;33:2091–2101.

651 50. Sharma L, Priya M, Bindumadhava H, Nair RM, Nayyar H. Influence of high temperature
652 stress on growth, phenology and yield performance of mungbean (*Vigna radiata* [L.]
653 Wilczek) under managed growth conditions. Sci Hortic. 2016;213:379–391.
654 doi:10.1016/j.scienta.2016.10.033.

655 51. Willits DH, Peet MM. Measurement of chlorophyll fluorescence as a heat stress indicator in
656 tomato: laboratory and greenhouse comparisons. J Am Soc Hortic Sci. 2001;126:188–194.

657 52. Camejo D, Rodríguez P, Morales A, Dell'Amico JM, Torrecillas J, Alarcón JJ. High
658 temperature effects on photosynthetic activity of two tomato cultivars with different heat
659 susceptibility. J Plant Physiol. 2005;162:281–289.

660 53. Liu X, Huang B. Heat stress injury in relation to membrane lipid peroxidation in creeping
661 bentgrass. Crop Sci. 2000;40:503–510.